Title

Spinal TLR4 mediates the transition to a persistent mechanical hypersensitivity after the resolution of inflammation in serum-transferred arthritis

Journal

Pain, 152(12)

ISSN

0304-3959

Authors

Christianson, Christina A
Dumlao, Darren S
Stokes, Jennifer A
et al.

Publication Date

2011-12-01

DOI

10.1016/j.pain.2011.09.020

Peer reviewed

Published in final edited form as:
Pain. 2011 December ; 152(12): 2881–2891. doi:10.1016/j.pain.2011.09.020.

Spinal TLR4 mediates the transition to a persistent mechanical hypersensitivity after the resolution of inflammation in serum-transferred arthritis

Christina A. Christianson[1,2], **Darren S. Dumlao**[3], **Jennifer A. Stokes**[1,2], **Edward A. Dennis**[2], **Camilla I. Svensson**[4], **Maripat Corr**[5], and **Tony L. Yaksh**[1,2]

[1]Department of Pharmacology, University of California, San Diego, La Jolla, California

[2]Department of Anesthesiology, University of California, San Diego, La Jolla, California

[3]Department of Chemistry and Biochemistry, University of California, San Diego La Jolla, California

[4]Department of Physiology and Pharmacology, Karolinska Institute, Stockholm, Sweden

[5]Division of Rheumatology, Allergy and Rheumatology, University of California, San Diego, La Jolla, California

Abstract

Persistent pain after resolution of clinically appreciable signs of arthritis poses a therapeutic challenge and immunosuppressive therapies do not meet this medical need. To investigate this conversion to persistent pain, we utilized the K/BxN serum transfer arthritis model, which has persistent mechanical hypersensitivity despite the resolution of visible inflammation. Toll-like receptor (TLR) 4 has been implicated as a potential therapeutic target in neuropathic and other pain models. We compared the relative courses of serum transfer arthritis and mechanical hypersensitivity in wild type (WT) and *Tlr4*$^{-/-}$ mice. K/BxN serum transfer induced similar joint swelling and inflammation from days 4–22 in WT and *Tlr4*$^{-/-}$ mice. Unlike WT mice, *Tlr4*$^{-/-}$ mice displayed a significant reversal in mechanical hypersensitivity and diminished appearance of glial activation markers after resolution of peripheral inflammation. Intrathecal (IT) delivery of a TLR4 antagonist, LPS-RS (10μg), on days 6, 9, and 12 abrogated the transition to persistent mechanical hypersensitivity in WT arthritic mice, while later administration had no impact. We utilized a lipodomics LC/MS/MS methodology to determine spinal cord profiles of bioactive lipid species following early LPS-RS treatment compared to vehicle treated controls. WT arthritic mice had reduced spinal levels of the anti-inflammatory prostaglandin 15d-PGJ_2 on day 6, compared to IT LPS-RS treated mice. Direct IT application of 15d-PGJ_2 (0.5μg) on day 6 improved mechanical hypersensitivity in arthritic mice within 15 minutes. Hence, TLR4 signaling altered spinal bioactive lipid profiles in the serum transfer model and played a critical role in the transition from acute to chronic post-inflammatory mechanical hypersensitivity.

Address Correspondence to: Tony L. Yaksh, Anesthesiology and Pharmacology University of California San Diego; San Diego, California; Tel: (619)543-3597; tyaksh@ucsd.edu.

The authors declare no conflicts of interest.

Keywords

arthritis; allodynia; astrocytes; microglia; inflammation; Toll-like receptor 4 (TLR4)

1. Introduction

Despite the efficacy of new small molecule and biologic treatment strategies in inflammatory arthritis, pain remains a significant clinical issue, and can persist after resolution of joint swelling [50]. Residual pain might be due to incompletely treated subclinical inflammation or irreversible articular tissue damage. Post-inflammatory pain might also be the result of a facilitated state of nociceptive processing at the level of the spinal dorsal horn, which would compel a separate therapeutic approach [48]. The presence of toll-like receptors (TLRs) in the spinal cord suggests the presence of central endogenous activators that could influence spinal nociceptive processing.

Amongst the TLRs, TLR4 has been described as a contributing receptor to both neuropathic pain and the perpetuation of peripheral joint inflammation in murine models of arthritis. TLR4 is extensively expressed on spinal microglia [24], astrocytes [7], and certain small primary afferent neurons [53]. Non-neuronal cells are critical in the development of facilitated pain states following inflammation and nerve injury (reviewed in [20,29,46,52]). In addition, nerve injury induced hypersensitivity is attenuated in *Tlr4*$^{-/-}$ mice and in mice treated with spinal TLR4 oligonucleotides [22,49]. Thus, while the TLRs were originally described according to their ability to respond to exogenous microbial products there is sufficient literature to suggest endogenous products activating TLRs during sterile inflammation. Prior work suggests that TLR4 recognizes not only lipopolysaccharide (LPS) [40], but also ligands arising from local tissues, including fibronectin A [34], heat shock protein (HSP)60 [32], HSP70 [4] and tenasacin-C [30].

A regulatory role for TLR4 has also been extensively investigated in murine models of arthritis initiated by a variety of innate and adaptive immune mechanisms, including IL-1Ra deficiency [2], intra-articular streptococcal cell wall (SCW) injection [1] and collagen induced arthritis [26]. The role of TLR4 in sustaining murine synovitis in the K/BxN serum transfer model was originally reported in C3H/HeJ mice, which are deficient in TLR4 signaling, and have an attenuated clinical course of K/BxN serum transferred arthritis [12]. In this model, transfer of antibodies against glucose-6-phosphate isomerase in the sera from K/BxN mice induces mechanical hypersensitivity in the recipient concurrent with the onset of inflammation. However, as we previously reported, after the clinical signs of paw and joint swelling resolve there is persistent mechanical hypersensitivity, which is reduced by gabapentin, but not by NSAID or peripherally restricted etanercept treatment [13].

In the present studies, we thus sought to investigate the role of TLR4 in the transition to a persistent pain-like behavior resulting from chronic inflammatory arthritis. Using *Tlr4*$^{-/-}$ mice and IT delivery of a TLR4 antagonist, LPS-RS, we demonstrated that the transition to persistent mechanical hypersensitivity was dependent upon spinal TLR4. Increased levels of mRNA transcripts of tenasacin C and heat shock protein (HSP)90, were detected in the spinal cords of arthritic mice. In addition, a lipidomic profile of spinal lipid mediators implicated a protective role for the anti-inflammatory protaglandin, 15-deoxy-$\Delta^{12,14}$ prostaglandin J_2 (15d- PGJ_2), in LPS-RS treated mice. Concordantly, IT administration of 15d- PGJ_2 transiently reversed mechanical hypersensitivity in arthritic WT mice.

2. Materials and Methods

2.1 Animals

Animal experiments were all conducted according to protocols approved by the Institutional Animal Care and Use Committee of the University of California San Diego. Mice were housed up to five per standard cage at room temperature and maintained on a 12 hour light/dark cycle. All behavioral testing was performed during the light cycle period. Both food and water were available *ad libitum.* Wild type C57Bl/6 (WT) mice (male 25–30g) were purchased from Harlan (Indianapolis, IN). KRN mice were a gift from Drs. D. Mathis and C. Benoist (Harvard Medical School, Boston, Massachusetts, USA) and Institut de Génénetique et de Biologie Moléculaire et Cellulaire (Strasbourg, France). These mice were maintained on a C57Bl/6 background (K/B). Arthritic mice were obtained by crossing K/B with NOD/Lt (N) animals (K/BxN). NOD/Lt mice were purchased from The Jackson Laboratory (Bar Harbor, Maine, USA). *Tlr4*$^{-/-}$ mice were provided by S. Akira (Osaka University, Osaka, Japan) and maintained on a C57Bl/6 background.

2.2 Serum transfer and arthritis scoring

Groups of adult arthritic K/BxN arthritic mice were bled, the sera pooled and transferred to recipient mice by intraperitoneal (i.p.) injection of 100μL sera on days 0 and 2. Animals received sera from single pool within an experiment, but different pools of sera were used between experiments. Clinical arthritis scores were evaluated, as described previously [12], using a scale of 0–4 for each paw with a higher number representing a greater disease progression with a total possible score of 16. Briefly, one point was given if swelling was observed for (i) any or all of the digits, (ii) the knuckles, (iii) the dorsal aspect of the paw and/or (iv) the ankle. Ankle thickness was measured with calipers in mm and compared to baseline thickness.

2.3 Drugs and drug delivery

Lipopolysaccharide (LPS, *Escherichia coli* 0111:B4) and the TLR4 antagonist LPS-RS (LPS *Rhodobacter sphaeroides*) were purchased from Invivogen, San Diego, CA. 15d-PGJ_2 (Caymen) was prepared in saline after the methyl acetate solvent was evaporated using a gentle argon stream. All IT injections were done under brief isoflourane anesthesia (2.5%) by lumbar puncture with a 30g needle attached to a Hamilton syringe. Normal saline was used as a vehicle control. LPS-RS (10μg), LPS (0.1μg), and 15d-PGJ_2 (0.5μg) were dissolved in normal saline and delivered in a 5μl volume. The LPS-RS, LPS, and 15d-PGJ_2 dosages were based upon previous studies [22,27,55] and preliminary dose ranging studies.

2.4 Behavioral tests

Animals were subjected to the thermal paw threshold test and the von Frey mechanical threshold test. Thermally evoked paw withdrawal responses were assessed using a Hargreaves-type testing device [15] (UARDG, Department of Anesthesiology, University of California, San Diego). This device consists of a glass surface (maintained at 30 °C) on which the mice rest in individual plexiglass cubicles. A thermal nociceptive stimulus originates from a focused projection bulb positioned below the glass surface. Latency was defined as the amount of time required for the mouse to produce a brisk withdrawal of the paw as detected by photodiode motion sensors that stop the timer and terminate the thermal stimulus.

Von Frey hairs ranging from 2.44 to 4.31 (0.03g to 2.00g) were applied to the rear hind paw using the up-down method as described previously [11]. The 50% probability withdrawal threshold (the force of the von Frey hair to which an animal reacts to 50% of the presentations) was recorded. Some data were also presented as the hyperalgesic index,

which represents the area under the time-effect curve after drug delivery in which the percentage change from baseline (e.g. arthritic state) threshold is plotted against time. The resulting value has the units percentage change × time. The formula for calculating the percentage change is 100 × (baseline threshold – post-drug threshold)/(baseline threshold), where the threshold was expressed in grams. Decreasing values indicate analgesic efficacy. The experimenter was blinded to drug treatments during all behavioral testing.

2.5 Histology

Whole ankle joint sections were fixed in formalin, decalcified, and embedded in paraffin. Sections were stained with hematoxylin and eosin (H&E) and Safranin O (HistoTox, Boulder, Colorado, USA). Histopathological evaluation was performed as previously described for inflammation, bone erosion and cartilage destruction [12].

2.6 Immunohistochemistry

At indicated time points, mice were deeply anesthetized with euthasol and perfused intracardially with 0.9% saline followed by 4% paraformaldehyde. The spinal cords were removed, post fixed, and cryoprotected in sucrose. Lumbar sections (L4–L6) of the spinal cord were cut on a microtome (30μm) as free floating sections. Tissue sections were incubated with anti-GFAP antibody (1:1000 Sigma, St. Louis MO) or anti-Iba1 antibody (1:1000 Wako, Richmond, VA). Binding sites were visualized with secondary antibodies conjugated with fluoro-Alexa-488 and Alexa-555 (1:500, Molecular Probes, Eugene, OR). Images were captured by Leica TCS SP5 confocal imaging system and quantified using Image-Pro Plus v.5.1 software.

The reactive state of glia was characterized by both an increase in the number of cells, and in the conformational changes of these cells (rounding of the cell bodies and thickening of processes) leading to an increase in antibody labeling with glia reactivity increases. Microglia (Iba1) and astrocyte (GFAP) staining was quantified by measuring the total integrated intensity of pixels divided by the total number of pixels in a standardized area of the dorsal horn. The investigator was blinded to experimental conditions during the quantification. Staining intensity was examined in lamina I-II of the superficial dorsal horn or of a standardized box in lamina V of the deeper dorsal horn region with 3 slices (separated by at least 180 μm) examined per animal and 3–6 animals per experimental condition. Only pixels above a preset background threshold were included. An increase in the integrated intensity / pixels for Iba1 and GFAP staining was interpreted to signify microglia and astrocyte reactivity, respectively. All data are presented as % change from the corresponding control group. Statistics were performed on raw data values.

2.7 Quantitative Real-time PCR (q-PCR)

The mRNA from flash frozen lumbar spinal cord was extracted using Trizol (Invitrogen) according to the manufacturer's protocol. Complementary DNA was prepared using MultiScribe reverse transcriptase (Applied Biosystems) and qPCR performed with TaqMan Universal PCR master mix and predesigned primer and probe sets (according to the manufacturer's instructions, Applied Biosystems Carlsbad, CA), using a GeneAmp 7500 Fast Sequence Detection system (Applied Biosystems). Pre-developed specific primers used included: tenascin-C (Assay ID: Mm00495662_m1), heat shock protein 90 (HSP90) (Assay ID: Mm00658568_gH), fibronectin (Assay ID: Mm01281423_m1) and HPRT1 (Assay ID Mm00446968_m1). Relative abundance was calculated by comparing Ct to a standard curve of cell equivalents [8] and the data were then normalized to HPRT1 mRNA levels to obtain relative gene expression units.

2.8 Liquid Chromatography and Mass Spectrometry

Isolated spinal cord samples were resuspended in 1 ml of 10% methanol and 50 μl of a 50 pg/μl solution of deuterated eicosanoid internal standards. The internal standard solution contained 50 pg/μL (2.5 ng total) of the following deuterated eicosanoids: (d_4) 6k $PGF_{1\alpha}$, (d_4) TXB_2, (d_4) $PGF_{2\alpha}$, (d_4) PGE_2, (d_4) PGD_2, (d_4) 15d PGJ_2, (d_{11}) 5-iso $PGF_{2\alpha}$ VI, (d_4) dhk $PGF_{2\alpha}$, (d_4) dhk PGE_2, (d_4) dhk PGD_2, (d_4) LTB_4, (d_8) 5-HETE, (d_8) 15-HETE, (d_6) 20-HETE, (d_4) 9-HODE, (d_4) 13-HODE, (d_7) 5-oxoETE, (d_8) 5, 6-EET, (d_8) 8, 9-EET, (d_8) 11, 12-EET, (d_8) 14, 15-EET, (d_4) 9, 10-diHOME, and (d_4) 12, 13-diHOME, (d_5) LTC_4, (d_4) LTE_4, and (d_4) AA. Cords were disrupted using a hand held sonicating probe for 6 s. Eicosanoids were extracted into 1 ml of methanol using solid-phase extraction columns (Phemononex, CA) as previously described [10]. Samples were then stored at −80°C until analyzed by the mass spectrometer. Samples were lyophilized to dryness using vacuum centrifugation, then resuspended in 100 μl of buffer A (30% acetonitrile, 70% water, 0.02% acetic acid; v/v/v). A 40 μl aliquot of sample was separated on a reverse-phase column (Phenomenex) with a 25 min HPLC gradient at 0.3 ml/min that consisted of: 1 min (0% B), 3 min (25% B), 11 min (45% B), 13 min (60% B), 18 min (75% B), 18.5 min (90% B), 20 min (90% B), 21 min (0% B), and 25 min (0% B). Buffer A consisted of 30% acetonitrile, 70% water, 0.02% acetic acid and buffer B consisted of 50% acetonitrile and 50% isopropanol; v/v/v. Eicosanoids were subsequently detected using a tandem quadrupole mass spectrometer (ABI 4000 Q-TrapR, Analyst 1.5 software, Applied Biosystems) via scheduled multiple reaction monitoring (sMRM) in negative-ion mode. The electrospray voltage was −4.5 kV, the turbo ion spray source temperature was 525°C. Collisional activation of eicosanoid precursor ions used nitrogen as a collision gas. Eicosanoids were identified in samples by matching their MRM signal and LC retention time with those of a pure standard.

Quantitation—Eicosanoids were quantitated using ABI's Multiquant 1.1 software. Quantitated values were determined from a stable isotope dilution method using pure eicosanoid standards [19]. All data was filtered using the Grubb's test to remove outliers. Quantitated averages were determined from treatment groups whose N ranged from 6 – 8 animals. Quantitated amounts are reported as pg/mg of tissue ± SEM. Significant metabolite changes (p value < 0.05) were determined using a two-tailed Students *t*-test. Supplementary table 1 details the average pg/mg of tissue for each eicosanoid investigated.

2.9 Statistics

Data are given as mean ± standard error. For comparison of changes in pain behavior (thermal and mechanical hypersensitivity) a two-way ANOVA for repeated measures with a Bonferroni *post hoc* test was used. For comparison of microglia and astrocyte changes and western blotting changes a one-way ANOVA with a Bonferroni *post hoc* test was used. For pairwise comparisons a Students *t* test was used.

3. Results

3.1 Post-inflammation mechanical hypersensitivity is TLR4 dependent in K/BxN serum transfer arthritis

Wild type C57Bl/6 (WT) and *Tlr4*$^{-/-}$ C57Bl/6 (*Tlr4*$^{-/-}$) mice were injected on days 0 and 2 with 100μl pooled K/BxN sera. Within 24 hours of serum transfer, WT mice developed significant clinical signs of arthritis (Figure 1A) including redness and paw swelling (Figure 1B) and mechanical hypersensitivity (Figure 1C), as previously described [13]. *Tlr4*$^{-/-}$ mice also developed clinical signs of arthritis (Figure 1A) and ankle swelling (Figure 1B), which were not significantly different than WT mice. Ankle joints were examined for histopathologic changes using H&E, and Safranin O staining. Joints were scored according to previous methods [12] for signs of inflammation, bone erosion, and cartilage destruction.

There were no significant differences in histological scores between WT (Figures 2A, B, C, and D) and *Tlr4*$^{-/-}$ arthritic mice (Figures 2E, F, G, and H) on days 0, 6 and 42.

WT and *Tlr4* $^{-/-}$ mice displayed equivalent mechanical hypersensitivity concurrent with signs of clinical arthritis. However, after the resolution of visible signs of inflammation from days 25–42, the WT mice demonstrated sustained mechanical hypersensitivity; whereas the *Tlr4*$^{-/-}$ mice returned to their baseline levels (Figure 1C, $p<0.001$). Consistent with previous studies, WT mice displayed a very modest thermal hypoalgesia (Figure 1D, $p<0.01$) during maximal inflammation. These results suggested that TLR4 was not required for the induction of acute inflammatory pain, but was required for the transition to chronic post inflammatory pain.

3.2 Reduction in spinal cord microglia and astrocyte activation in arthritic *Tlr4*$^{-/-}$ mice compared to WT

The complete resolution of the post-inflammation mechanical hypersensitivity in the *Tlr4*$^{-/-}$ mice compared to the WT mice suggested that there might be differences in activation of microglia and astrocytes at the spinal cord level. Chronic pain is frequently accompanied by and thought to be regulated by glia activation [5,18]. Hence, we examined the activation of astrocytes and microglia by histological markers GFAP and Iba1, respectively. Protein expression levels for microglia (Iba1) and astrocytes (GFAP) were assessed from L4-L6 of the superficial dorsal horn and deeper dorsal horn using immunoreactivity. The average of WT naïve densitometry scores were set to 100% and changes in densitometry scoring of staining were expressed as a percent change from WT naïve values. In general, WT animals showed an increase in dorsal horn astrocyte and microglia signals on day 6, which was numerically less in *Tlr4*$^{-/-}$ mice (Figure 3A and C). (Microglia at 6 days in WT vs *Tlr4*$^{-/-}$: 138 ±18% vs. 80 ± 10%; $p<0.05$%; Astrocytes at 6 days in WT vs. *Tlr4*$^{-/-}$: 335 ±22 vs 278 ±34%; $p>0.05$%).

At the later time point, day 42, the microglia signal in *Tlr4*$^{-/-}$ animals as compared to WT was not statistically significant (WT vs. *Tlr4*$^{-/-}$: 84 ± 15% vs43% ± 2%; $p>0.05$). In contrast, astrocyte staining relative to naïve baseline levels was more highly elevated in the WT as compared to the *Tlr4*$^{-/-}$ (257 ± 14% vs. 189 ±11%; $p<0.05$%).

3.3 Intrathecal activation of TLR4 induces acute and chronic mechanical hypersensitivity with activation of microglia and astrocytes

To confirm pain-like behavior resulting from spinal TLR4 activation, mice were injected IT with 0.1μg of lipopolysaccharide (LPS), which specifically signals via TLR4 [41]. LPS induced mechanical hypersensitivity in WT but not *Tlr4*$^{-/-}$ mice from 30 minutes to 7 days following injection, $p<0.05$-0.001 (Figure 4A). Baseline values dropped in WT mice from 1.62g (± 0.16g) to between 0.19g (± 0.03) and 0.36g (±0.08g) following LPS delivery. A significant increase in pain-like behavior occurred only in WT mice following IT LPS delivery (Figure 4B; $p<0.01$ vs. IT saline (WT) and $p<0.001$ vs IT LPS (*Tlr4*$^{-/-}$).

We next determined if intrathecal TLR4 activation by LPS (0.1μg) induced spinal dorsal horn (L4-L6) microglia (Iba1) and astrocyte (GFAP) activation via changes in immunoreactivity. The average densitometry score (integrated intensity) of IT saline for each time point of interest (4 hours or 7 days) was established as 100% and changes in densitometry staining were reported as a percent change compared to IT saline control values. Astrocyte (GFAP) and microglia (Iba1) immunoreactivity in the superficial dorsal horn showed a significant increase 4 hours post IT LPS, but not 7 days post IT LPS, compared to control ($p<0.05$; Figure 4C and D respectively). Densitometry indicated that immunostaining of microglia and astrocytes were not significantly increased at day 7.

Representative images for astrocytes (GFAP staining; Figure 4E) and microglia (Iba1 staining; Figure 4F) 4 hours and 7 days following IT saline and IT LPS are shown.

3.4 TLR4 ligand mRNA levels are elevated in arthritic spinal cords during the post-inflammation phase

Although IT administration of the microbially derived TLR4 ligand LPS induced mechanical hypersensitivity (Figure 4A), a centrally acting endogenous ligand was more likely to be involved in the arthritis model. We investigated the mRNA transcript levels of several previously described TLR4 ligands: HSP90, tenascin-C and fibronectin in the spinal cord by qPCR. All expression levels were measured in the lumbar spinal cord on day 42 during the post-inflammation period when WT arthritic mice no longer displayed clinical signs, but persistent mechanical hypersensitivity was present. Tenascin-C has recently been demonstrated to be a TLR4 ligand that is upregulated in the joints during rheumatoid arthritis [30]. Here we show an increase of tenascin-C in the spinal cords of mice 2.57 ± 0.1 vs 3.88 ± 0.3 REU in control vs. arthritic mice respectively, $p<0.05$ (Figure 5A). HSP90 has been demonstrated to contribute to TLR4 mediated mechanical hypersensitivity [21]. Here we show an increase of HSP90 of 16.08± 3.3 vs. 32.98± 6.1REU in control vs. arthritic mice respectively, $p<0.05$ (Figure 5B). However, there was no difference in the transcript levels of fibronectin 0.67± 0.1 vs. 0.81± 0.1 REU in control vs. arthritic mice respectively, $p>0.05$ (Figure 5C).

3.5 IT TLR4 antagonism during the peak inflammation prevents post-inflammation persistent mechanical hypersensitivity

To determine the spinal involvement of TLR4 during the inflammation to post-inflammation transition WT arthritic mice were given three IT injections of the TLR4 antagonist LPS-RS (10μg) or three IT injections of saline either early or late in the course of arthritis. IT LPS-RS delivered on days 6, 9, and 12 during the inflammation period significantly reduced the mechanical hypersensitivity on day 15 – 28; $p<0.05$-0.001 (Figure 6A) as compared to IT saline injections. Although the hypersensitivity was reduced 2 hours post IT injection on days 6 and 9, the nociception returned in the interim period, thus requiring additional treatment. Clinical scores (Figure 6B) and changes in ankle widths (Figure 6C) were not affected by LPS-RS delivery on day 6, 9, and 12. IT LPS-RS delivered on days 18, 21, and 24 during the post-inflammation period did not impact the persistent mechanical hypersensitivity present (Figure 6D), clinical scores (Figure 6E) or ankle widths (Figure 6F) as compared to IT saline treatments.

3.6 Peripheral inflammation from K/BxN serum transfer arthritis induces central changes to the spinal eicosanoid profile

We were interested in understanding how K/BxN serum transfer arthritis would affect the central eicosanoid profile. These lipid products have been previously characterized to play an important role in regulating the sensitivity of sensory neurons both peripherally and in the spinal cord during peripheral inflammation [6]. The lumbar enlargement of the spinal cord was removed and analyzed for eicosanoid levels from three experimental groups; A) non-arthritic mice 2 hours after an IT saline injection, B) arthritic mice 2 hours after an IT saline injection and C) arthritic mice 2 hours after an IT TLR4 antagonist injection (10μg LPS-RS) on day 6 post-arthritis induction.

Eicosanoids were measured and quantified using a stable isotope dilution technique coupled with a liquid chromatography tandem mass spectrometry (LC/MS/MS) method operating in selected multiple reaction monitoring (sMRM) mode [6]. We detected and quantified 60 lipid metabolites out of 139 total metabolites monitored using individually optimized sMRM pairs, which are summarized in supplementary table 1. Significant differences ($p < 0.5$)

between the eicosanoids produced were determined using the Students *t*-test. Twenty-six of the 60 detected eicosanoids were significantly different when non-arthritic (IT saline injected) control mice were compared to K/BxN induced arthritic (IT saline injected) mice. Only 11 significantly different eicosanoids were detected between arthritic IT saline and IT LPS-RS treated mice.

The data are shown in a heat map in order to view the global changes to the eicosanoid profile between non-arthritic and arthritic IT saline treated groups (Figure 7A and 7C). Eicosanoids were clustered based on their biosynthetic pathway. K/BxN serum transfer arthritis induced the production of eicosanoids from the 5-, 12-, 15-lipoxygenase (LOX), cytochrome P450 (CYP), and non-enzymatic pathways. Central cyclooxygenase (COX) metabolites remained largely unaffected, although K/BxN arthritic mice had reduced levels of 15d-PGJ_2, a dehydration product of PGD_2.

Few changes in the eicosanoid profile were detected when comparing arthritic + IT saline and arthritic + IT LPS-RS treated mice (Figure 7B and 7D). Intrathecal LPS-RS treatment rapidly improved mechanical hypersensitivity and caused reduced amounts of LOX degradation (HEDH) and CYP metabolites. Interestingly, PGD_2 dehydration products (15d-PGD_2, PGJ_2, and 15d-PGJ_2) increased with LPS-RS treatment. These results suggest that blocking TLR4 activation with LPS-RS treatment caused 15d-PGJ_2 levels to return to normal.

On day 6 the spinal cords of non-arthritic IT saline injected mice had PGE_2 values of 70.1 (± 8.6 SEM) pg/mg of tissue. In comparison, day 6 arthritic mice 2 hours after IT treatment of saline had an average PGE_2 value of 82.7 (± 7.4) pg/mg of tissue and those after 10μg of LPS-RS had an average value of 102.9 (± 5.0) pg/mg of tissue ($p<0.05$ vs arthritic saline treated; Figure 8A). The levels of PGD_2 and of 15k- PGE_2, the PGE_2 enzymatic breakdown product, were not significantly different (Figure 8B and C). This indicates that PGE_2 may not be the predominant factor in TLR4 mediated mechanical hypersensitivity.

While PGD_2 levels were not significantly different between the three treatment groups (Figure 8B), a significant change was detected for the non-enzymatic breakdown product of PGD_2, 15-deoxy-PGJ_2. Non-arthritic saline treated mice had an average value of 0.95 (± 0.2) pg/mg of tissue which dropped significantly in the spinal cords of IT saline treated arthritic mice to 0.57 (±0.1) pg/mg of tissue ($p<0.05$) and recovered to 1.69 (± 0.2) pg/mg of tissue, higher than baseline values following IT LPS-RS treated ($p<0.05$; Figure 8D). These findings are in accordance with the known role for 15-deoxy-PGJ_2 as an anti-inflammatory mediator [16,17,45].

3.8 Intrathecal delivery of the TLR4 antagonist LPS-RS during the inflammation period replenishes 15d-PGJ_2, reduced by arthritis

To determine if 15d-PGJ_2 would attenuate the nociception prominent during the inflammation period of K/BxN serum transfer arthritis we delivered 0.5μg IT on day 6. Arthritic mice with an average baseline of 0.23g ± 0.08 displayed a transient recovery of mechanical hypersensitivity to 1.05g± 0.2 15 minutes after intrathecal delivery of 15d-PGJ_2 as compared to saline vehicle treated mice (Figure 8E; $p<0.05$). Evidence indicates that 15d-PGJ_2 can directly activate the TRPA1 receptor [25], therefore non-arthritic mice were also injected as a control. At the given dose, these mice displayed no significant changes as compared to pre-injection baselines over the two hour time course. Drug efficacy was also quantified according to the hyperalgesic index, where IT 15d-PGJ_2 treated mice displayed significant analgesic activity ($p<0.05$) in comparison to saline treated vehicle controls according to this measure (Figure 8F).

Discussion

K/BxN serum transfer arthritis has revealed that similar to clinical arthritis a persistent pain condition exists, even after resolution of synovitis [13]. This model recapitulates some, but not all aspects of human rheumatoid arthritis. Using the K/BxN model, we have previously shown that the persistent mechanical hypersensitivity outlasting the clinical signs of arthritis was associated with ATF-3 activation in the dorsal root ganglia (DRG). The expression of this transcription factor has been taken to be a DRG marker reflecting changes resembling those evoked by nerve injury. These results led to the hypothesis that during the course of this persistent, but slowly resolving inflammatory state there is a transition to a neuropathic phenotype. Examining the pharmacology of this pain state, we have shown that while the early (inflammatory) phase of pain-like behavior was responsive to a NSAID (ketorolac), gabapentin, and to peripherally restricted TNF blockade (Etanercept), reversal of the late phase pain response was limited to gabapentin. These findings further suggested a transition from an inflammatory to a neuropathic pain state [13]. Here we show that activation of spinal TLR4 contributes to the continuation of mechanical hypersensitivity during the transition from the acute peripheral inflammatory phase to the post-inflammatory phase of K/BxN serum transfer arthritis.

Current evidence supports a role for the innate immune system, in particular TLRs during glial activation in the central nervous system following peripheral insult [23]. Specifically TLR4 has been detected on both microglia and astrocytes [9]. In the present study we demonstrated that during K/BxN serum transfer arthritis progression, a constitutive TLR4 deletion attenuated increased spinal astrocyte and microglia immunoreactivity.

Whereas IT TLR4 antagonism reduced mechanical hypersensitivity, it had no impact upon peripheral arthritis. In contrast to a prior report of K/BxN serum transfer arthritis [12] we did not detect a significant difference in clinical scores or peripheral pathology between WT and TLR4 signaling deficient arthritic mice. There were differences in the strains used however, as the previous study utilized the C3H/HeJ mouse, which has a spontaneous mutation in *Tlr4* rendering the protein functionally inactive. In the C3H/HeJ mouse the signaling inactive molecule could be providing a separate scaffolding function that is not present in the TLR4 null model. During the inflammation period in our study, maximal inflammation scores were achieved by both genotypes making differences in clinical scores difficult to ascertain.

TLR4 activation couples to NF-κB through two distinct pathways. It can induce a myeloid differentiation primary response gene 88 (MyD88) dependent cascade leading to early NF-κB activation and subsequent upregulation or activation of cytokines including TNF, IL-18 and enzymes such as cyclooxygenase-2, p38, and c-Jun-N-terminal kinases (JNK). The second cascade is TIR-domain-containing adapter-inducing interferon-β (TRIF) dependent leading to delayed NF-κB activation and interferon-β production (reviewed in [36]). Many of the cytokines produced in response to TLR4 activation are also known to be pro-nociceptive and contribute to spinal sensitization [28,29,44]. Earlier work has shown that spinal NF-κB was important in both inflammatory and nerve injury-induced pain [25] and of particular interest, direct blockade of NFκB activity in astrocytes attenuate mechanical hypersensitivity and release of chemokines including CCL2 and CXCL10 following chronic constriction injury of the sciatic nerve [16].

Although TLR4 is the receptor for LPS, TLR4, is also activated by endogenous ligands (reviewed in [14,31,42]). Spinal cord mRNA changes clearly indicate a role for intrinsic TLR4 ligands released during chronic arthritis. Researchers have identified a diverse groups of endogenous TLR4 ligands including heat shock proteins 60 [33], 70 [54], and 90 [38], fibrinogen [47], fibronectin [35,43], hyaluronic acid [51], HMGB1 [37], and tenascin-C

[30]. Many of these ligands have been identified as contributing to the inflammation and cartilage destruction in the joint during inflammatory arthritis, thus supporting a role for TLR4 during this disease. Spinal cord mRNA changes observed in the present work clearly indicate a role spinally for intrinsic TLR4 ligands released during chronic arthritis. While human and animal models suggest a peripheral function, this was the first study examining TLR4 expression and endogenous activation during inflammatory arthritis in the central nervous system.

A role for endogenous TLR4 ligands was further supported by the utilization of IT LPS-RS, a TLR4 antagonist. A single dose of IT LPS-RS when delivered during the inflammation period will reverse mechanical hypersensitivity within two hours. Three doses delivered during the inflammation period will prevent the transition to persistent hypersensitivity. The elevated transcripts for endogenous TLR4 ligands suggested that there is persistent central TLR4 stimulation in the post-inflammatory phase on day 42. However, intrathecal LPS-RS during the post-inflammation phase was ineffective. In contrast, a previous report indicated that a single dose of IT LPS-RS in rats rapidly and effectively reversed neuropathic pain for three hours resulting from a chronic constriction injury to the nerve [22]. This may reflect some element distinguishing the events secondary to chronic inflammation as compared to a frank mechanical nerve injury. However, the lack of a response to the later delivery of IT LPS-RS suggested a role for TLR4 in the transition phase that is not required to manifest the chronic neuropathic phase of this model.

As TLR4 antagonism was only effective in the acute phase of the arthritis in preventing prolonged hypersensitivity, we investigated potential mediators on day 6 in the spinal cord. There are many potential mechanisms that might be involved. However, in a recent study of murine Lyme arthritis, the lipid mediator profiles temporally co-varied with inflammation [6]. Of note, different patterns were observed between the susceptible strain, C3H/HeJ which has a point mutation in *Tlr4* as compared to the arthritis resistant strain, DBA [6]. Hence, we focused our study on profiling the bioactive lipids in the spinal cord at a critical time prior to the transition period.

The levels of 15-deoxy-$\Delta^{12,14}$-PGJ_2 (15d-PGJ_2) were relatively reduced in WT mice with arthritis compared to normal controls. The spinal cord levels of 15d-PGJ_2 in arthritic mice treated with IT LPS-RS were similar to non-arthritic mice. Prostaglandins (PGs) such as 15-deoxy-$\Delta^{12,14}$-PGJ_2 (15d-PGJ_2) are electrophilic lipid signaling mediators derived from the nonenzymatic dehydration of PGD_2, a major product of the cyclooxygenase pathway. The biological actions of 15d-PGJ_2 are attributed to its ability to form covalent adducts with thiol residues within specific signaling proteins, thus triggering redox-sensitive cell signaling pathways [39]. Indeed, direct IT delivery of this prostaglandin transiently reduced pain in the K/BxN model. A continual production in the spinal cord would be needed, however, to have a sustained response.

Peripheral delivery of TLR4 antagonists reduced inflammation and cartilage destruction during inflammatory arthritis [3] and spinal administration mitigated neuropathic pain following chronic constriction injury [22]. Of note, this was the first report demonstrating that spinal injection of TLR4 antagonists attenuated inflammatory arthritis induced pain-like behavior. We have demonstrated a link between TLR4 mediated nociception during the inflammation phase of K/BxN serum transfer arthritis and the establishment of a persistent pain state. The robustness of the effects of blocking TLR4 function either by genetic manipulation or biochemical antagonism emphasizes the contribution of spinal systems in processing that leads to a persistent pain condition, particularly in the observed absence of prominent changes in the inflammatory stimulus as reported here. Furthermore, the bioactive eicosanoid 15-deoxy-PGJ_2 levels fluctuated concurrently with arthritis initiation and TLR4

inhibition. It remains to be tested whether central or peripheral delivery of anti-inflammatory mediators in this pathway are more effective. Defining this underlying linkage may be critical for understanding the persistency of the pain state in chronic inflammatory conditions. These data provides an exciting potential mechanism for future experimental work and therapeutic investigations regarding TLR4 actions during transitional phases of chronic inflammation.

Supplementary Material

Refer to Web version on PubMed Central for supplementary material.

Acknowledgments

This work was supported by grants from the National Institutes of Health (NS16541, and DA02110, TLY; GM064611, and GM069338, ED; 2T32GM007752-31 JS and CC), the Arthritis Foundation (MC) and the Swedish Research Council (CIS), Swedish Foundation for Strategic Research (CIS), ScanDesign International Association for Studies of Pain (CIS, TLY), Marie Curie International Reintegration grant (CIS), Olle Engkvist Byggmästares Foundation (CIS).

References

1. Abdollahi-Roodsaz S, Joosten LA, Helsen MM, Walgreen B, van Lent PL, van den Bersselaar LA, Koenders MI, van den Berg WB. Shift from toll-like receptor 2 (TLR-2) toward TLR-4 dependency in the erosive stage of chronic streptococcal cell wall arthritis coincident with TLR-4-mediated interleukin-17 production. Arthritis Rheum. 2008; 58(12):3753–3764. [PubMed: 19035506]
2. Abdollahi-Roodsaz S, Joosten LA, Koenders MI, Devesa I, Roelofs MF, Radstake TR, Heuvelmans-Jacobs M, Akira S, Nicklin MJ, Ribeiro-Dias F, van den Berg WB. Stimulation of TLR2 and TLR4 differentially skews the balance of T cells in a mouse model of arthritis. J Clin Invest. 2008; 118(1): 205–216. [PubMed: 18060042]
3. Abdollahi-Roodsaz S, Joosten LA, Roelofs MF, Radstake TR, Matera G, Popa C, van der Meer JW, Netea MG, van den Berg WB. Inhibition of Toll-like receptor 4 breaks the inflammatory loop in autoimmune destructive arthritis. Arthritis Rheum. 2007; 56(9):2957–2967. [PubMed: 17763416]
4. Asea A, Rehli M, Kabingu E, Boch JA, Bare O, Auron PE, Stevenson MA, Calderwood SK. Novel signal transduction pathway utilized by extracellular HSP70: role of toll-like receptor (TLR) 2 and TLR4. J Biol Chem. 2002; 277(17):15028–15034. [PubMed: 11836257]
5. Austin PJ, Moalem-Taylor G. The neuro-immune balance in neuropathic pain: involvement of inflammatory immune cells, immune-like glial cells and cytokines. J Neuroimmunol. 229(1–2):26–50. [PubMed: 20870295]
6. Blaho VA, Buczynski MW, Brown CR, Dennis EA. Lipidomic analysis of dynamic eicosanoid responses during the induction and resolution of Lyme arthritis. J Biol Chem. 2009; 284(32):21599–21612. [PubMed: 19487688]
7. Bowman CC, Rasley A, Tranguch SL, Marriott I. Cultured astrocytes express toll-like receptors for bacterial products. Glia. 2003; 43(3):281–291. [PubMed: 12898707]
8. Boyle DL, Rosengren S, Bugbee W, Kavanaugh A, Firestein GS. Quantitative biomarker analysis of synovial gene expression by real-time PCR. Arthritis Res Ther. 2003; 5(6):R352–360. [PubMed: 14680510]
9. Bsibsi M, Ravid R, Gveric D, van Noort JM. Broad expression of Toll-like receptors in the human central nervous system. J Neuropathol Exp Neurol. 2002; 61(11):1013–1021. [PubMed: 12430718]
10. Buczynski MW, Svensson CI, Dumlao DS, Fitzsimmons BL, Shim JH, Scherbart TJ, Jacobsen FE, Hua XY, Yaksh TL, Dennis EA. Inflammatory hyperalgesia induces essential bioactive lipid production in the spinal cord. J Neurochem. 114(4):981–993. [PubMed: 20492349]
11. Chaplan SR, Bach FW, Pogrel JW, Chung JM, Yaksh TL. Quantitative assessment of tactile allodynia in the rat paw. J Neurosci Methods. 1994; 53(1):55–63. [PubMed: 7990513]

12. Choe JY, Crain B, Wu SR, Corr M. Interleukin 1 receptor dependence of serum transferred arthritis can be circumvented by toll-like receptor 4 signaling. J Exp Med. 2003; 197(4):537–542. [PubMed: 12591910]

13. Christianson CA, Corr M, Firestein GS, Mobargha A, Yaksh TL, Svensson CI. Characterization of the acute and persistent pain state present in K/BxN serum transfer arthritis. Pain. 151(2):394–403. [PubMed: 20739123]

14. Cristofaro P, Opal SM. Role of Toll-like receptors in infection and immunity: clinical implications. Drugs. 2006; 66(1):15–29. [PubMed: 16398566]

15. Dirig DM, Salami A, Rathbun ML, Ozaki GT, Yaksh TL. Characterization of variables defining hindpaw withdrawal latency evoked by radiant thermal stimuli. J Neurosci Methods. 1997; 76(2): 183–191. [PubMed: 9350970]

16. Fu ES, Zhang YP, Sagen J, Candiotti KA, Morton PD, Liebl DJ, Bethea JR, Brambilla R. Transgenic inhibition of glial NF-kappa B reduces pain behavior and inflammation after peripheral nerve injury. Pain. 148(3):509–518. [PubMed: 20097004]

17. Gilroy DW, Colville-Nash PR, Willis D, Chivers J, Paul-Clark MJ, Willoughby DA. Inducible cyclooxygenase may have anti-inflammatory properties. Nat Med. 1999; 5(6):698–701. [PubMed: 10371510]

18. Gosselin RD, Suter MR, Ji RR, Decosterd I. Glial cells and chronic pain. Neuroscientist. 16(5): 519–531. [PubMed: 20581331]

19. Hall LM, Murphy RC. Electrospray mass spectrometric analysis of 5-hydroperoxy and 5-hydroxyeicosatetraenoic acids generated by lipid peroxidation of red blood cell ghost phospholipids. J Am Soc Mass Spectrom. 1998; 9(5):527–532. [PubMed: 9879367]

20. Hansson E, Ronnback L. Glial neuronal signaling in the central nervous system. FASEB J. 2003; 17(3):341–348. [PubMed: 12631574]

21. Hutchinson MR, Ramos KM, Loram LC, Wieseler J, Sholar PW, Kearney JJ, Lewis MT, Crysdale NY, Zhang Y, Harrison JA, Maier SF, Rice KC, Watkins LR. Evidence for a role of heat shock protein-90 in toll like receptor 4 mediated pain enhancement in rats. Neuroscience. 2009; 164(4): 1821–1832. [PubMed: 19788917]

22. Hutchinson MR, Zhang Y, Brown K, Coats BD, Shridhar M, Sholar PW, Patel SJ, Crysdale NY, Harrison JA, Maier SF, Rice KC, Watkins LR. Non-stereoselective reversal of neuropathic pain by naloxone and naltrexone: involvement of toll-like receptor 4 (TLR4). Eur J Neurosci. 2008; 28(1): 20–29. [PubMed: 18662331]

23. Jack CS, Arbour N, Manusow J, Montgrain V, Blain M, McCrea E, Shapiro A, Antel JP. TLR signaling tailors innate immune responses in human microglia and astrocytes. J Immunol. 2005; 175(7):4320–4330. [PubMed: 16177072]

24. Laflamme N, Rivest S. Toll-like receptor 4: the missing link of the cerebral innate immune response triggered by circulating gram-negative bacterial cell wall components. FASEB J. 2001; 15(1):155–163. [PubMed: 11149903]

25. Ledeboer A, Gamanos M, Lai W, Martin D, Maier SF, Watkins LR, Quan N. Involvement of spinal cord nuclear factor kappaB activation in rat models of proinflammatory cytokine-mediated pain facilitation. Eur J Neurosci. 2005; 22(8):1977–1986. [PubMed: 16262636]

26. Lee EK, Kang SM, Paik DJ, Kim JM, Youn J. Essential roles of Toll-like receptor-4 signaling in arthritis induced by type II collagen antibody and LPS. Int Immunol. 2005; 17(3):325–333. [PubMed: 15684036]

27. Materazzi S, Nassini R, Andre E, Campi B, Amadesi S, Trevisani M, Bunnett NW, Patacchini R, Geppetti P. Cox-dependent fatty acid metabolites cause pain through activation of the irritant receptor TRPA1. Proc Natl Acad Sci U S A. 2008; 105(33):12045–12050. [PubMed: 18687886]

28. McMahon SB, Cafferty WB, Marchand F. Immune and glial cell factors as pain mediators and modulators. Exp Neurol. 2005; 192(2):444–462. [PubMed: 15755561]

29. McMahon SB, Malcangio M. Current challenges in glia-pain biology. Neuron. 2009; 64(1):46–54. [PubMed: 19840548]

30. Midwood K, Sacre S, Piccinini AM, Inglis J, Trebaul A, Chan E, Drexler S, Sofat N, Kashiwagi M, Orend G, Brennan F, Foxwell B. Tenascin-C is an endogenous activator of Toll-like receptor 4

that is essential for maintaining inflammation in arthritic joint disease. Nat Med. 2009; 15(7):774–780. [PubMed: 19561617]

31. Mollen KP, Anand RJ, Tsung A, Prince JM, Levy RM, Billiar TR. Emerging paradigm: toll-like receptor 4-sentinel for the detection of tissue damage. Shock. 2006; 26(5):430–437. [PubMed: 17047512]
32. Ohashi K, Burkart V, Flohe S, Kolb H. Cutting edge: heat shock protein 60 is a putative endogenous ligand of the toll-like receptor-4 complex. J Immunol. 2000; 164(2):558–561. [PubMed: 10623794]
33. Ohashi K, Burkart V, Flohe S, Kolb H. Cutting edge: heat shock protein 60 is a putative endogenous ligand of the toll-like receptor-4 complex. J Immunol. 2000; 164(2):558–561. [PubMed: 10623794]
34. Okamura Y, Watari M, Jerud ES, Young DW, Ishizaka ST, Rose J, Chow JC, Strauss JF 3rd. The extra domain A of fibronectin activates Toll-like receptor 4. J Biol Chem. 2001; 276(13):10229–10233. [PubMed: 11150311]
35. Okamura Y, Watari M, Jerud ES, Young DW, Ishizaka ST, Rose J, Chow JC, Strauss JF 3rd. The extra domain A of fibronectin activates Toll-like receptor 4. J Biol Chem. 2001; 276(13):10229–10233. [PubMed: 11150311]
36. Palsson-McDermott EM, O'Neill LA. Signal transduction by the lipopolysaccharide receptor, Toll-like receptor-4. Immunology. 2004; 113(2):153–162. [PubMed: 15379975]
37. Park JS, Svetkauskaite D, He Q, Kim JY, Strassheim D, Ishizaka A, Abraham E. Involvement of toll-like receptors 2 and 4 in cellular activation by high mobility group box 1 protein. J Biol Chem. 2004; 279(9):7370–7377. [PubMed: 14660645]
38. Peetermans WE, Raats CJ, Langermans JA, van Furth R. Mycobacterial heat-shock protein 65 induces proinflammatory cytokines but does not activate human mononuclear phagocytes. Scand J Immunol. 1994; 39(6):613–617. [PubMed: 8009177]
39. Perez-Sala D, Cernuda-Morollon E, Pineda-Molina E, Canada FJ. Contribution of covalent protein modification to the antiinflammatory effects of cyclopentenone prostaglandins. Ann N Y Acad Sci. 2002; 973:533–536. [PubMed: 12485923]
40. Poltorak A, He X, Smirnova I, Liu MY, Huffel CV, Du X, Birdwell D, Alejos E, Silva M, Galanos C, Freudenberg M, Ricciardi-Castagnoli P, Layton B, Beutler B. Defective LPS signaling in C3H/HeJ and C57BL/10ScCr mice: mutations in Tlr4 gene. Science. 1998; 282(5396):2085–2088. [PubMed: 9851930]
41. Poltorak A, He X, Smirnova I, Liu MY, Van Huffel C, Du X, Birdwell D, Alejos E, Silva M, Galanos C, Freudenberg M, Ricciardi-Castagnoli P, Layton B, Beutler B. Defective LPS signaling in C3H/HeJ and C57BL/10ScCr mice: mutations in Tlr4 gene. Science. 1998; 282(5396):2085–2088. [PubMed: 9851930]
42. Rossignol DP, Lynn M. TLR4 antagonists for endotoxemia and beyond. Curr Opin Investig Drugs. 2005; 6(5):496–502.
43. Saito S, Yamaji N, Yasunaga K, Saito T, Matsumoto S, Katoh M, Kobayashi S, Masuho Y. The fibronectin extra domain A activates matrix metalloproteinase gene expression by an interleukin-1-dependent mechanism. J Biol Chem. 1999; 274(43):30756–30763. [PubMed: 10521465]
44. Schaible HG, Richter F, Ebersberger A, Boettger MK, Vanegas H, Natura G, Vazquez E, Segond von Banchet G. Joint pain. Exp Brain Res. 2009; 196(1):153–162. [PubMed: 19363606]
45. Scher JU, Pillinger MH. 15d-PGJ2: the anti-inflammatory prostaglandin? Clin Immunol. 2005; 114(2):100–109. [PubMed: 15639643]
46. Scholz J, Woolf CJ. The neuropathic pain triad: neurons, immune cells and glia. Nat Neurosci. 2007; 10(11):1361–1368. [PubMed: 17965656]
47. Smiley ST, King JA, Hancock WW. Fibrinogen stimulates macrophage chemokine secretion through toll-like receptor 4. J Immunol. 2001; 167(5):2887–2894. [PubMed: 11509636]
48. Sokka T, Kautiainen H, Toloza S, Makinen H, Verstappen SM, Lund Hetland M, Naranjo A, Baecklund E, Herborn G, Rau R, Cazzato M, Gossec L, Skakic V, Gogus F, Sierakowski S, Bresnihan B, Taylor P, McClinton C, Pincus T. QUEST-RA: quantitative clinical assessment of

patients with rheumatoid arthritis seen in standard rheumatology care in 15 countries. Ann Rheum Dis. 2007; 66(11):1491–1496. [PubMed: 17412740]

49. Tanga FY, Nutile-McMenemy N, DeLeo JA. The CNS role of Toll-like receptor 4 in innate neuroimmunity and painful neuropathy. Proc Natl Acad Sci U S A. 2005; 102(16):5856–5861. [PubMed: 15809417]
50. Taylor PC. The importance of the patients' experience of RA compared with clinical measures of disease activity. Clin Exp Rheumatol. 28(3 Suppl 59):S28–31. [PubMed: 20576222]
51. Termeer C, Benedix F, Sleeman J, Fieber C, Voith U, Ahrens T, Miyake K, Freudenberg M, Galanos C, Simon JC. Oligosaccharides of Hyaluronan activate dendritic cells via toll-like receptor 4. J Exp Med. 2002; 195(1):99–111. [PubMed: 11781369]
52. Tsuda M, Inoue K, Salter MW. Neuropathic pain and spinal microglia: a big problem from molecules in "small" glia. Trends Neurosci. 2005; 28(2):101–107. [PubMed: 15667933]
53. Wadachi R, Hargreaves KM. Trigeminal nociceptors express TLR-4 and CD14: a mechanism for pain due to infection. J Dent Res. 2006; 85(1):49–53. [PubMed: 16373680]
54. Wang Y, Kelly CG, Singh M, McGowan EG, Carrara AS, Bergmeier LA, Lehner T. Stimulation of Th1-polarizing cytokines, C-C chemokines, maturation of dendritic cells, and adjuvant function by the peptide binding fragment of heat shock protein 70. J Immunol. 2002; 169(5):2422–2429. [PubMed: 12193710]
55. Wu HE, Sun HS, Cheng CW, Terashvili M, Tseng LF. dextro-Naloxone or levo-naloxone reverses the attenuation of morphine antinociception induced by lipopolysaccharide in the mouse spinal cord via a non-opioid mechanism. Eur J Neurosci. 2006; 24(9):2575–2580. [PubMed: 17100845]

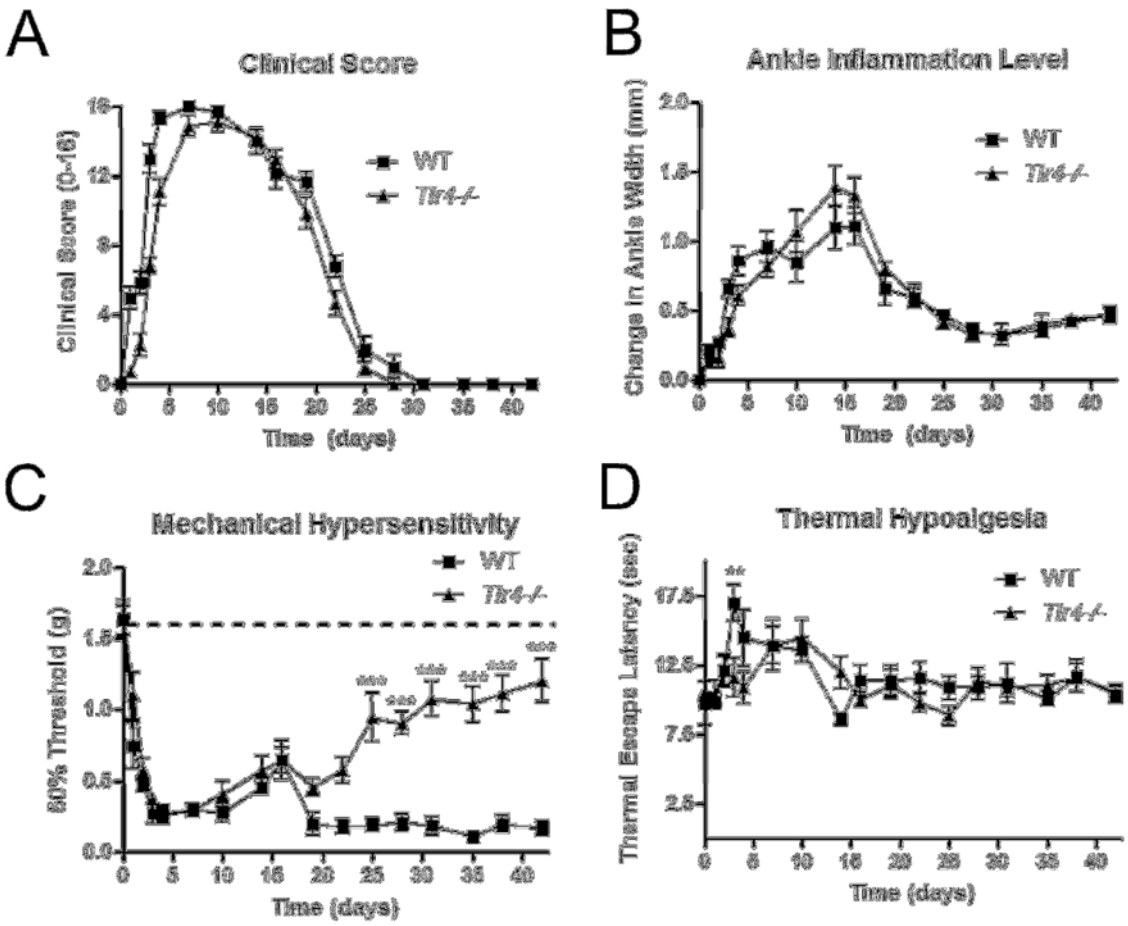

Figure 1.

TLR4 was required to maintain mechanical hypersensitivity in the post inflammation stage of K/BxN serum transfer arthritis. Graphs displaying (A) ankle thickness as measured using calipers and (B) clinical scores indicate no significant differences between WT and *Tlr4*$^{-/-}$ during the progression of K/BxN serum transfer arthritis. (C) Tactile thresholds (g) indicate significant mechanical hypersensitivity day 2–21 for WT and *Tlr4*$^{-/-}$ mice compared to baseline levels, as marked by the dotted line at 1.55g on the graph. *Tlr4*$^{-/-}$ mice displayed significant improvements in mechanical hypersensitivity as compared to time matched WT mice days 24–42. (D) WT mice displayed significant thermal hyposensitivity compared to *Tlr4*$^{-/-}$ mice only on day 3. Each time point represents mean ± SEM (n=9 mice/group), ***= p<0.001 by Bonferroni post-test.

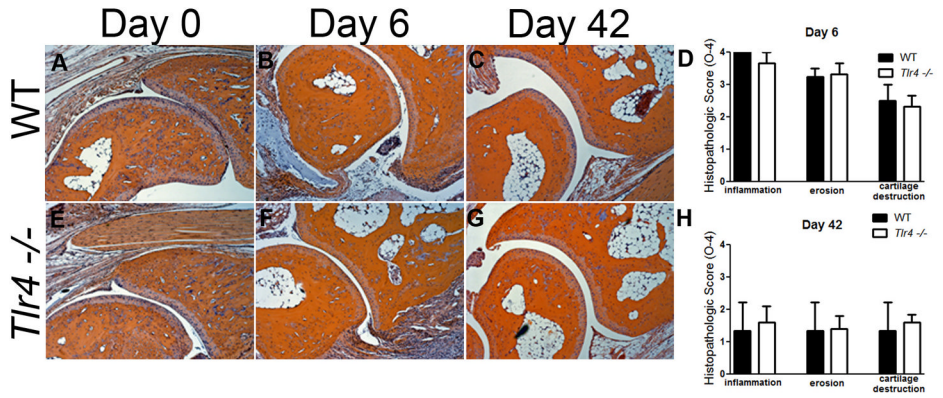

Figure 2.

K/BxN serum transfer induced peripheral joint histopathology in WT and *Tlr4*$^{-/-}$ mice. (A) Mice were sacrificed 0, 6 and 42 days after arthritis induction and the ankle joints were removed, prepared for histology, sectioned and stained with H&E. x40 original magnification. WT (B) and *Tlr4*$^{-/-}$ (C) arthritic mice have prominent inflammation, erosion, and cartilage destruction at day 6 and day 42 which are not statistically different between genotypes.

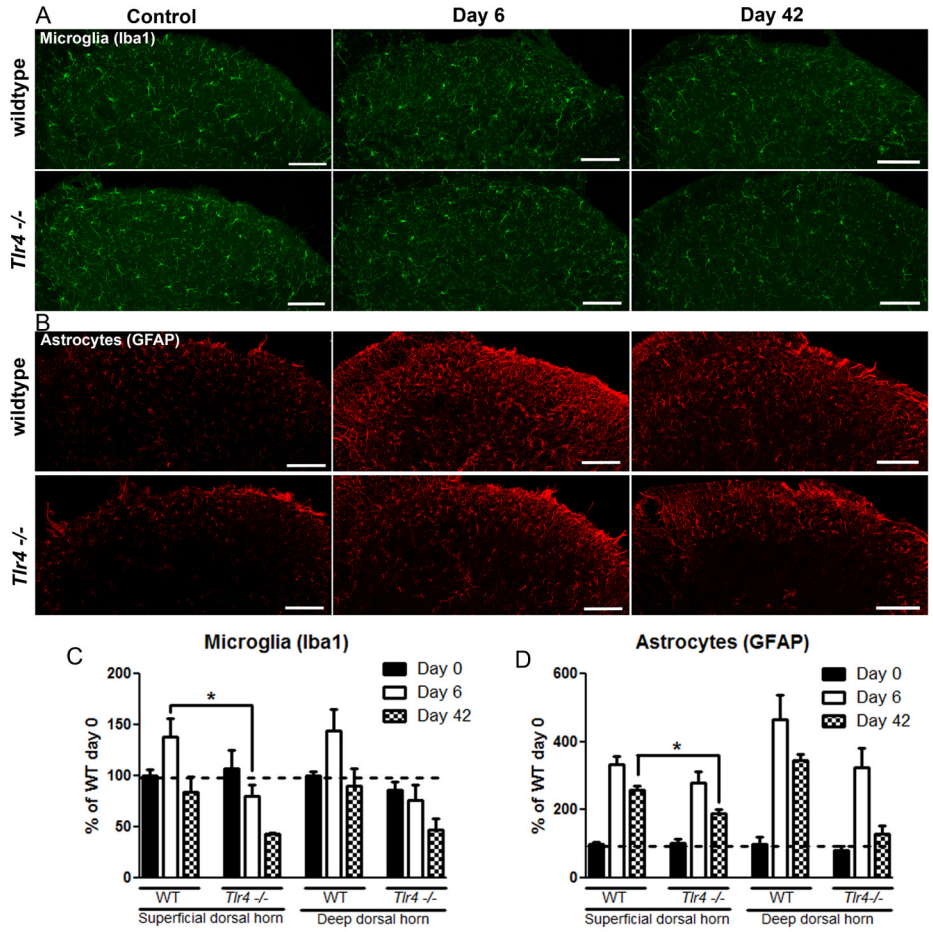

Figure 3.

Spinal immunohistochemistry of microglia (Iba1) and astrocytes (GFAP) from the dorsal horn of WT and *Tlr4*$^{-/-}$ mice 0, 6, and 42 days after K/BxN serum transfer arthritis induction. (A) Dorsal horn Iba-1 staining was increased at day 6 in WT, but not *Tlr4*$^{-/-}$ mice. (B) Dorsal horn GFAP staining was increased in WT and *Tlr4*$^{-/-}$ mice at day 6 and day 42. Densitometry indicates that WT mice increase Iba-1 immunoreactivity (C) and GFAP immunoreactivity (D) to a greater degree following K/BxN serum transfer than do *Tlr4*$^{-/-}$mice compared to naïve. Quantification of images was shown by densitometry (using integrated intensity). Scale bars: 50μm. *= $p<0.05$, ***=$p<0.001$ by Bonferroni post test. All experiments n= 3 mice, 3 sections per mouse. Representative sections shown.

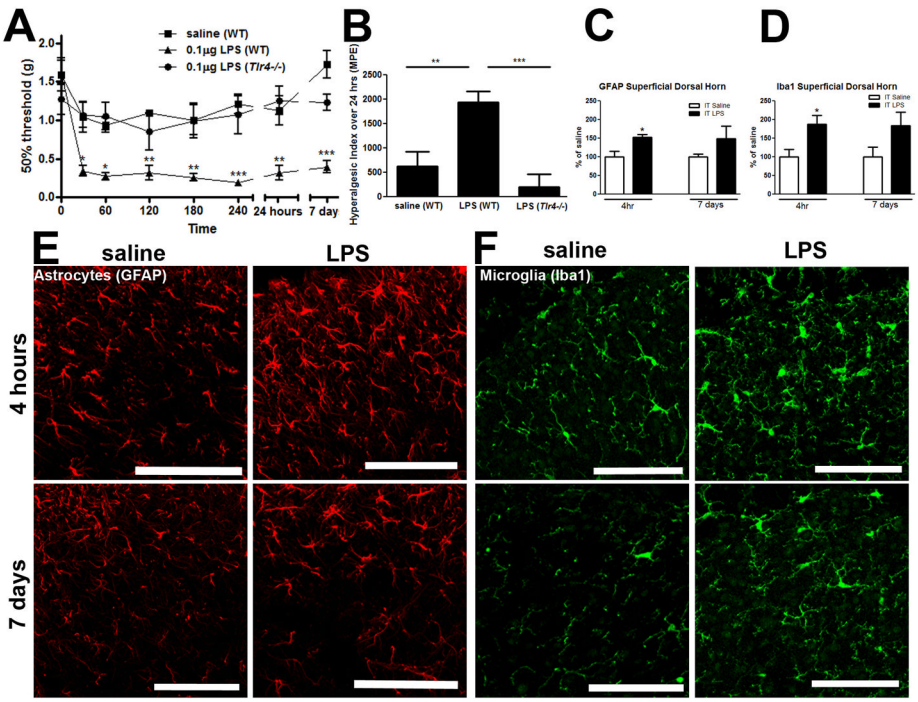

Figure 4.

Intrathecal activation of TLR4 produced mechanical hypersensitivity. (A) IT LPS (0.1μg) produced mechanical hypersensitivity (30 minutes to 7 days) in WT, but not *Tlr4* $^{-/-}$ mice or in WT saline treated mice, which was visualized in (B) by the hyperalgesic index. (C) Astrocyte staining (GFAP) was increased in the spinal dorsal horn 4hr after IT LPS, which was visualized in (E). (D) Microglia staining (Iba1) was increased in the spinal dorsal horn 4 hr after IT LPS, which was visualized in (F). Each time point represents mean ± SEM (n=6 mice/group), *= $p<0.05$, **= $p<0.01$, and ***= $p<0.001$ by Bonferroni post-test. Scale bars= 50μm.

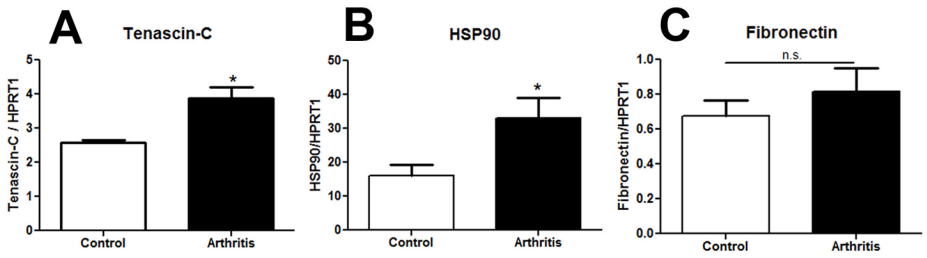

Figure 5.

Elevated levels of mRNA transcripts for reported TLR4 endogenous protein ligands in the spinal cord of arthritic mice. Spinal cords were removed on day 42 from arthritic mice and mice that received WT control sera. The mRNA was extracted and levels were assessed by qPCR. Relative expression units were normalized to HPRT1 levels. There were higher levels for tenascin-C (A) and HSP90 (B), but not fibronectin (C) in the spinal cords of d42 WT arthritic mice as compared to control serum treated animals. Each group represents mean ± SEM (n=5–6 mice/group), *=$p<0.05$ by Students *t*-test.

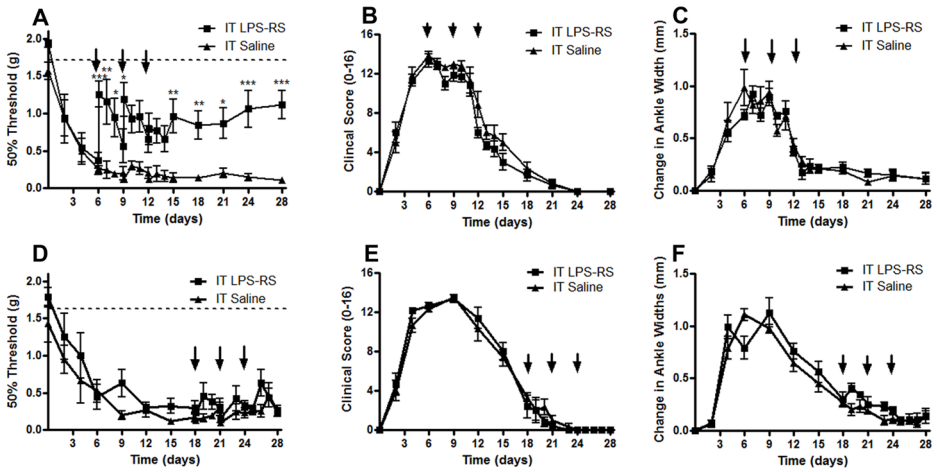

Figure 6.

Intrathecal (IT) delivery of a TLR4 antagonist (LPS-RS) during the inflammation period but not during the post-inflammation period of WT mice improved mechanical hypersensitivity without altering peripheral signs of inflammation. IT delivery of LPS-RS (10μg) on days 6, 9, and 12 post K/BxN serum transfer in WT mice (A) significantly improved mechanical hypersensitivity 2 hours after injection on days 6 and 9, and on days 7, 8, 15, 18, 21, 24, and 28 (C), but did not significantly affect ankle width and (F) clinical scores as compared to arthritic animals treated IT with saline. IT delivery of LPS-RS (10μg) on days 18, 21, and 24 post-K/BxN serum transfer in WT mice did not significantly alter (B) mechanical hypersensitivity (D) ankle width or (F) clinical scores as compared to IT saline. Each group represents mean ± SEM (n=4–6 mice/group), *=p<0.05, **= p<0.01, and ***=p<0.001 by Bonferroni post-test.

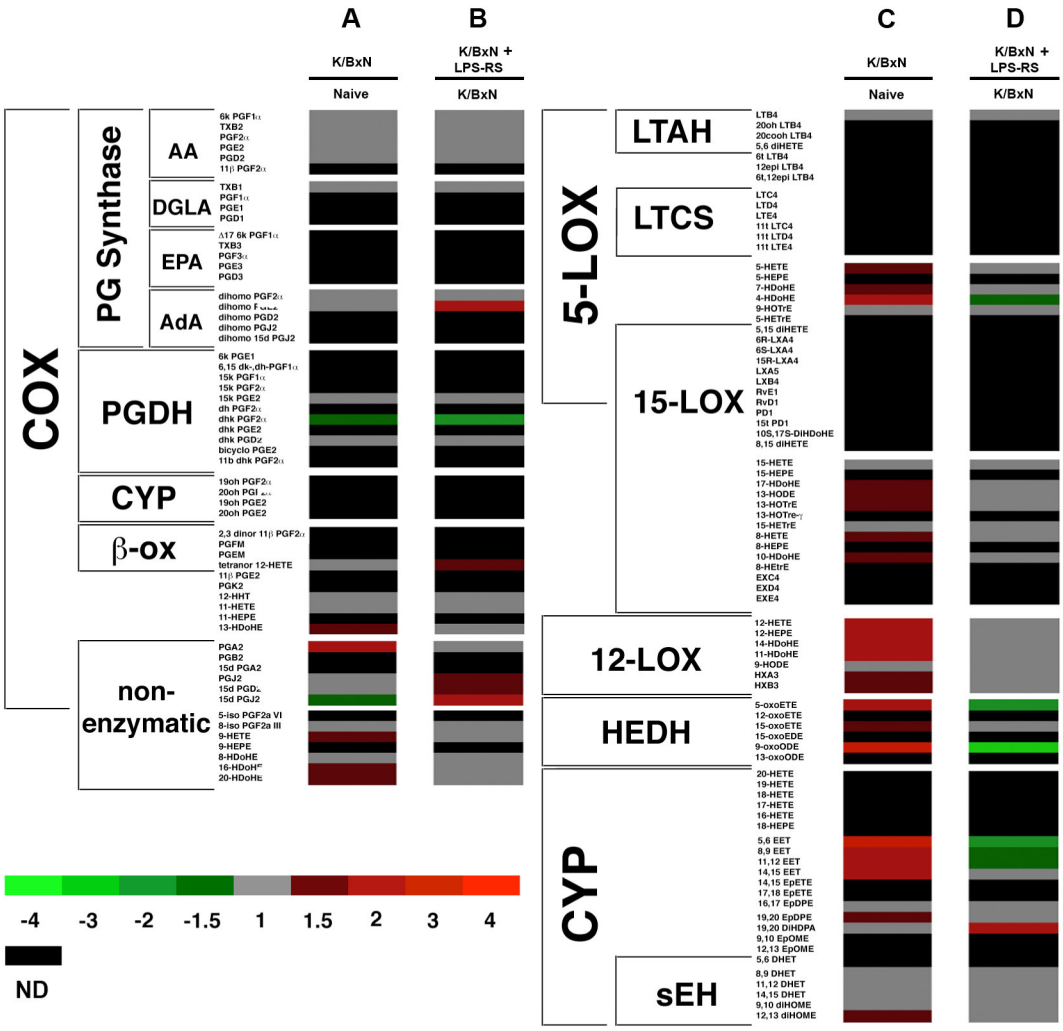

Figure 7.

Heat map displaying the relative fold-changes in the eicosanoid profile. (A and C) The changes in the eicosanoid profile in day 6 K/BxN serum transfer arthritic mice with respect to non-arthritic control mice. (B and D) A direct comparison between the relative eicosanoid levels detected in the lumbar spinal cords of day 6 arthritic mice treated with IT LPS-RS vs day 6 arthritic mice treated with IT saline. Columns A and B display COX products while C and D display LOX and CYP products. This analysis was determined from non-arthritic control (n=8), arthritic + IT saline (n=7), and arthritic + IT LPS-RS (n=8) mice. ND (black) indicates that the eicosanoid was either not detected or below our level of detection.

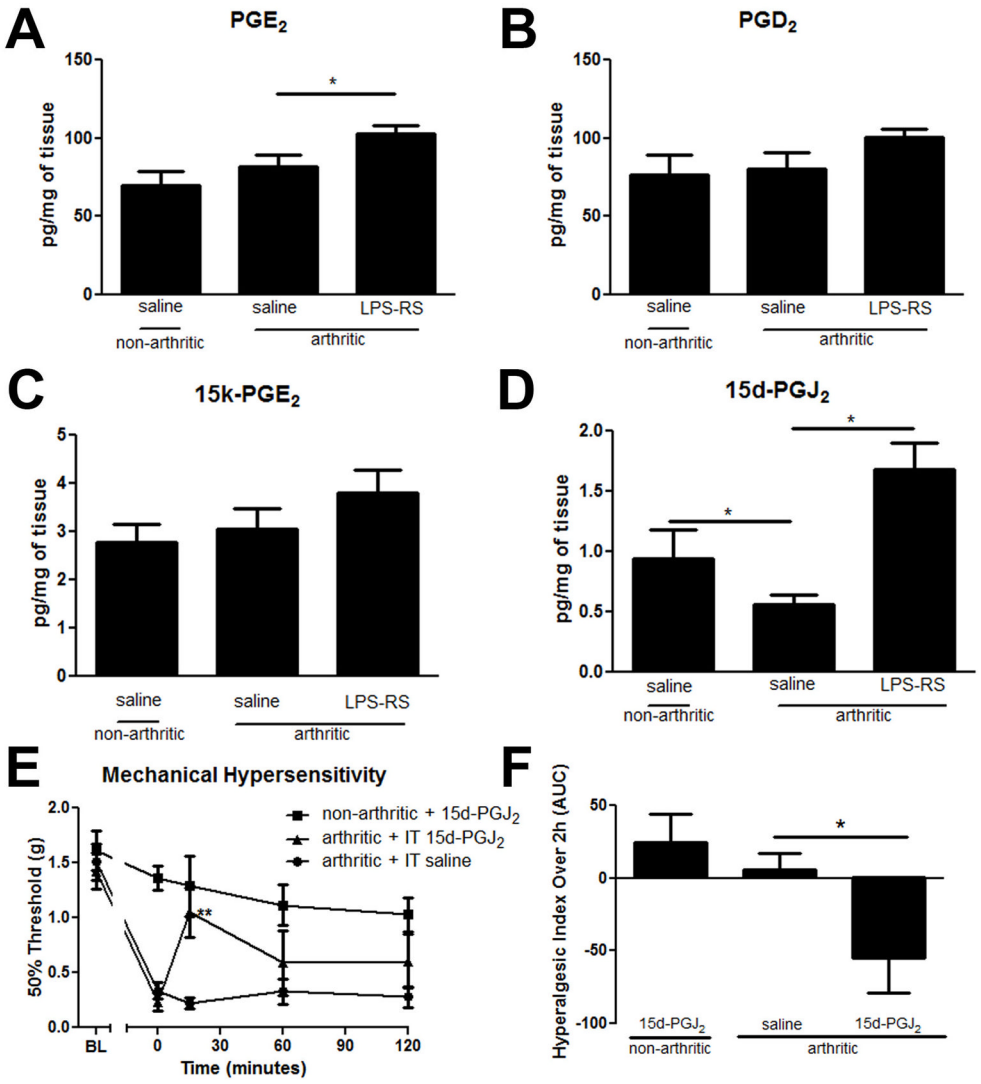

Figure 8.

Effects of arthritis and IT LPS-RS administration on PGE_2 and PGD_2 and their breakdown products of 15-keto-PGE_2 and 15-deoxy-PGJ_2 in the spinal cord on day 6, 2 hours after drug delivery. (A) PGE_2 was significantly increased 2 hours after IT LPS-RS treatment vs. IT saline in arthritic mice. (B) There are no significant changes in PGD_2 levels across treatment groups. (C) There were no significant changes in 15-keto-PGE_2 (PGE_2 enzymatic breakdown product) levels across treatment groups ($p>0.05$). (D) 15-deoxy-PGJ_2 was significantly decreased on day 6 in arthritic vs. non-arthritic mice 2 hours after having both received IT saline injections ($p<0.05$). This decrease was significantly recovered in arthritic mice 2 hours after administration of IT LPS-RS (10μg). (E) Mechanical hypersensitivity was significantly improved 15 minutes after IT delivery of 15d-PGJ_2 on day 6 K/BxN serum transfer arthritis which is presented according to the hyperalgesic index across the 2 hours post-delivery (F). Each group represents mean ± SEM (n=8 mice/group: mass spectrometry; n=5 mice/group: behavior), *=$p<0.05$ by Bonferroni post-test.